Available online at www.sciencedirect.com
SCIENCE DIRECT
Earth and Planetary Science Letters 241 (2006) 323–335
EPSL
www.elsevier.com/locate/epsl

Tertiary strike-slip faulting in southeastern Mongolia and implications for Asian tectonics

L.E. Webb [a,*], C.L. Johnson [b]

[a] Department of Earth Sciences, 204 Heroy Geology Laboratory, Syracuse University Syracuse, NY 13244, USA
[b] Department of Geology and Geophysics, 135 South 1460 East, WBB 609, University of Utah, Salt Lake City, UT 84112, USA

Received 30 March 2005; received in revised form 24 October 2005; accepted 25 October 2005
Available online 5 December 2005
Editor: R.D. van der Hilst

Abstract

Geologic maps have long portrayed the Late Cretaceous–Recent geologic history of southeastern Mongolia as tectonically quiescent. We present new data based on outcrop observations that indicate the northeast-trending East Gobi fault zone (EGFZ) was reactivated in the Cenozoic as a sinistral strike-slip fault system. Inversions of Cenozoic fault-slip data imply that faulting was associated with north–northwest subhorizontal shortening and east–northeast subhorizontal extension. We propose that faulting is Tertiary in age based on published interpretations of seismic reflection data which reveal that the mid-Cretaceous (~100–95 Ma) unconformity is deformed by strike-slip faults, and based on field observation of strike-slip faults and fracture sets that cut Upper Cretaceous and Cenozoic strata but lack evidence for neotectonic activity. Published seismicity maps also appear to argue against significant Quaternary faulting within the EGFZ. These new data may lend credence to published models proposing a Middle Miocene or older kinematic linkage between the EGFZ and the Altyn Tagh fault in China. The recognition that the EGFZ has a history of left-lateral displacement in both the Early Mesozoic and Cenozoic means that currently available estimates of offset based on displaced Paleozoic rocks constrain total offset only. This reactivation history supports the notion that inherited lithospheric structures are important in controlling the location and, thus, modes of intracontinental deformation in Asia as a function of collisional far field effects and evolving boundary conditions of the Pacific margin.

Keywords: intraplate deformation; strike-slip faults; fault reactivation; Asian tectonics; Cenozoic

1. Introduction

Northeast-trending faults define a structural corridor traceable for more than 300 km along strike through the center of the East Gobi basin in southeastern Mongolia (Figs. 1 and 2). This corridor, the East Gobi Fault Zone (EGFZ), has occupied an intraplate position since Late Paleozoic time [1,2]. At least three phases of Mesozoic reactivation of the EGFZ are evident in regional studies, including Late Triassic ductile sinistral shear [3], Early Cretaceous extension [4], and mid-Cretaceous basin inversion [5]. Nevertheless, the record of deformation along the EGFZ – particularly its most recent activation – is poorly understood.

This manuscript presents new data documenting Cenozoic strike-slip faulting. Neotectonic strike-slip faulting is well established in southwestern Mongolia [6,7], but southeastern Mongolia is thought to have been relatively stable since the Late Cretaceous: regional geologic maps show Upper Cretaceous post-rift strata

* Corresponding author. Fax: +1 315 443 3363.
E-mail addresses: lewebb@syr.edu (L.E. Webb), cjohnson@earth.utah.edu (C.L. Johnson).

0012-821X/$ - see front matter © 2005 Elsevier B.V. All rights reserved.
doi:10.1016/j.epsl.2005.10.033

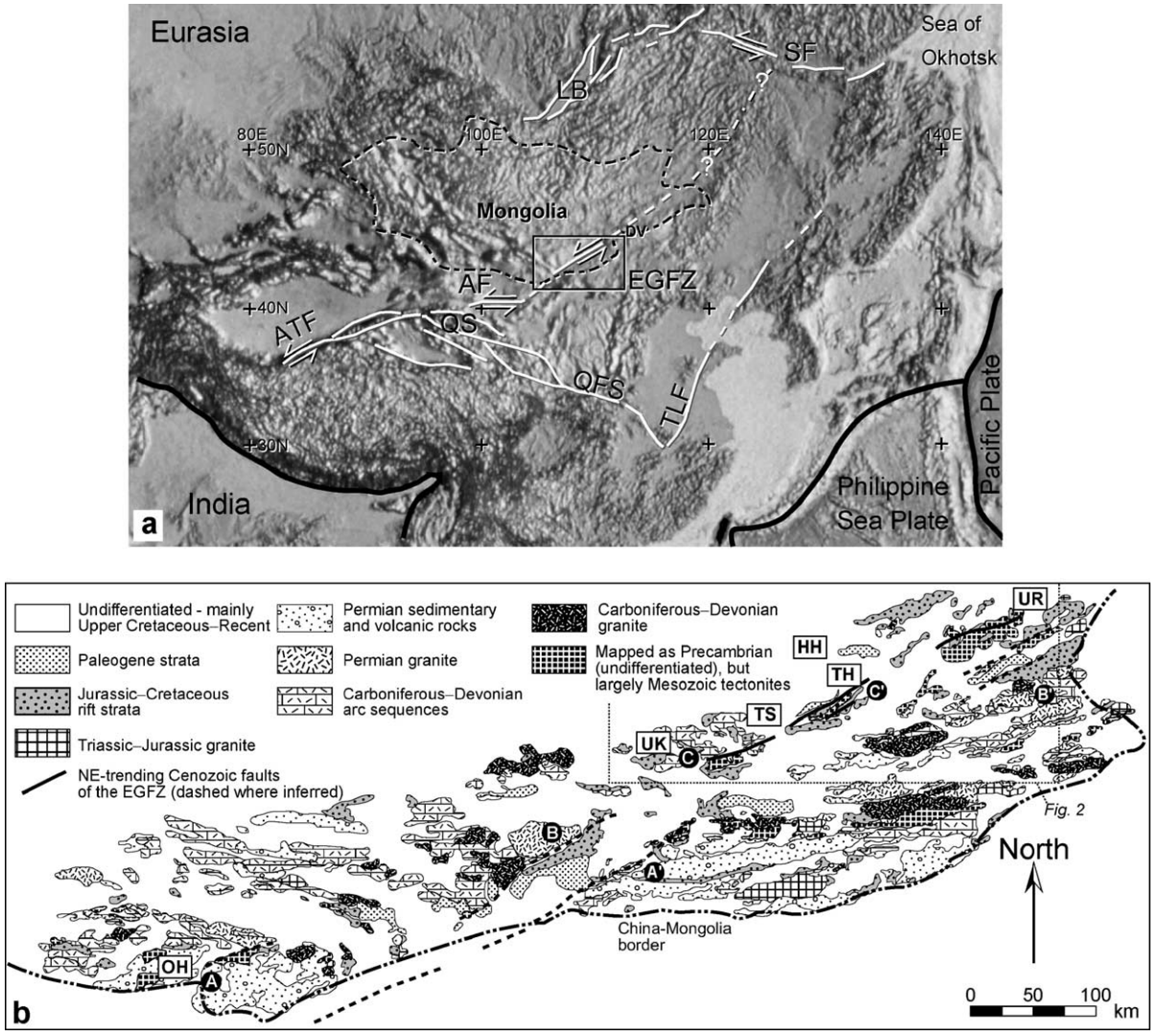

Fig. 1. a) Regional map showing major tectonic elements of China and Mongolia relevant to this study. Primary plate boundaries are shown in black and regional faults in white. Rectangle denotes area shown in b. AF = Alxa fault system, ATF = Altyn Tagh fault, DV = Dariganga volcanic field, EGFZ = East Gobi Fault zone, LB = Lake Baikal, QFS = Qinling fault system, QS = Qilian Shan, SF = Stanovoy fault system, TLF = Tan Lu fault. b) Simplified geologic map of southeastern Mongolia based and modified after Tomurtogoo [8]. Abbreviations for localities discussed in the text are as follows: OH = Onch Hayrhan, UK = Ulgay Khid, TS = Tsagan Subarga, HH = Har Hotol, TH = Tavan Har; UR = Urgun. The map shows possible offset markers across the EGFZ. A–A′ and B–B′ correspond to markers N–N′ and K–K′ from Fig. 2 of Lamb et al. [3], respectively, suggesting 185–235 km of total offset since the Paleozoic. C–C′ represents possible offset Lower Cretaceous lacustrine units that suggest up to 150 km of left-lateral offset may be attributed to Cenozoic strike-slip faulting.

overlapping most regional faults [8]. Recent studies in the East Gobi basin have proposed the existence of post-Cretaceous faults based on seismic reflection and limited outcrop data [5,9]. This work represents the first time that Cenozoic faults have been studied rigorously in outcrop and placed into a regional tectonic framework. The record of deformation in southeastern Mongolia reflects the growth and tectonic evolution of the Asian continent, and data from the EGFZ are critical for evaluating end-member models for continental deformation associated with the Indo-Asia collision (e.g., [10,11]).

1.1. Regional geology and inherited structural framework

First-order structural and basin analysis studies of southeastern Mongolia reveal distinct tectonic events postdating Late Paleozoic arc accretion and continental amalgamation (e.g., [4,12]). In each of these

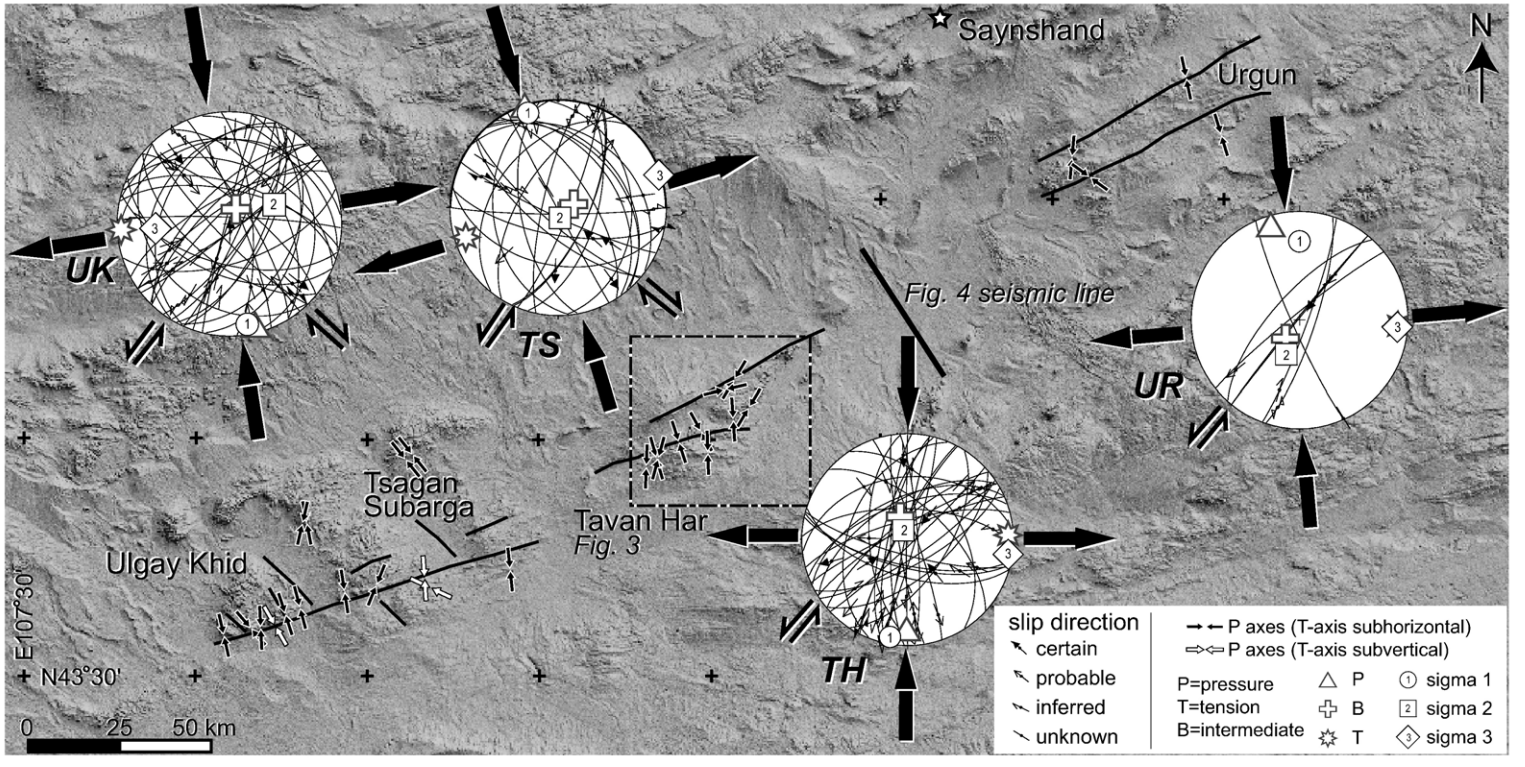

Fig. 2. Digital elevation model of the study area with vertical exaggeration of 15. Traces of major Cenozoic faults in field area are shown as black lines. Localities in which fault-slip data were collected are indicated by arrows that show map projection of calculated shortening directions (PBT *P*-axes; please see Methods section in text for full explanation of fault-slip data). Stereonets show Cenozoic fault-slip data and analytical results for the four main basement blocks. UK = Ulgay Khid, TS = Tsagan Subarga, TH = Tavan Har; UR = Urgun. Latitude–longitude grid (+ symbol) is shown in 30 min intervals (reference point at lower left).

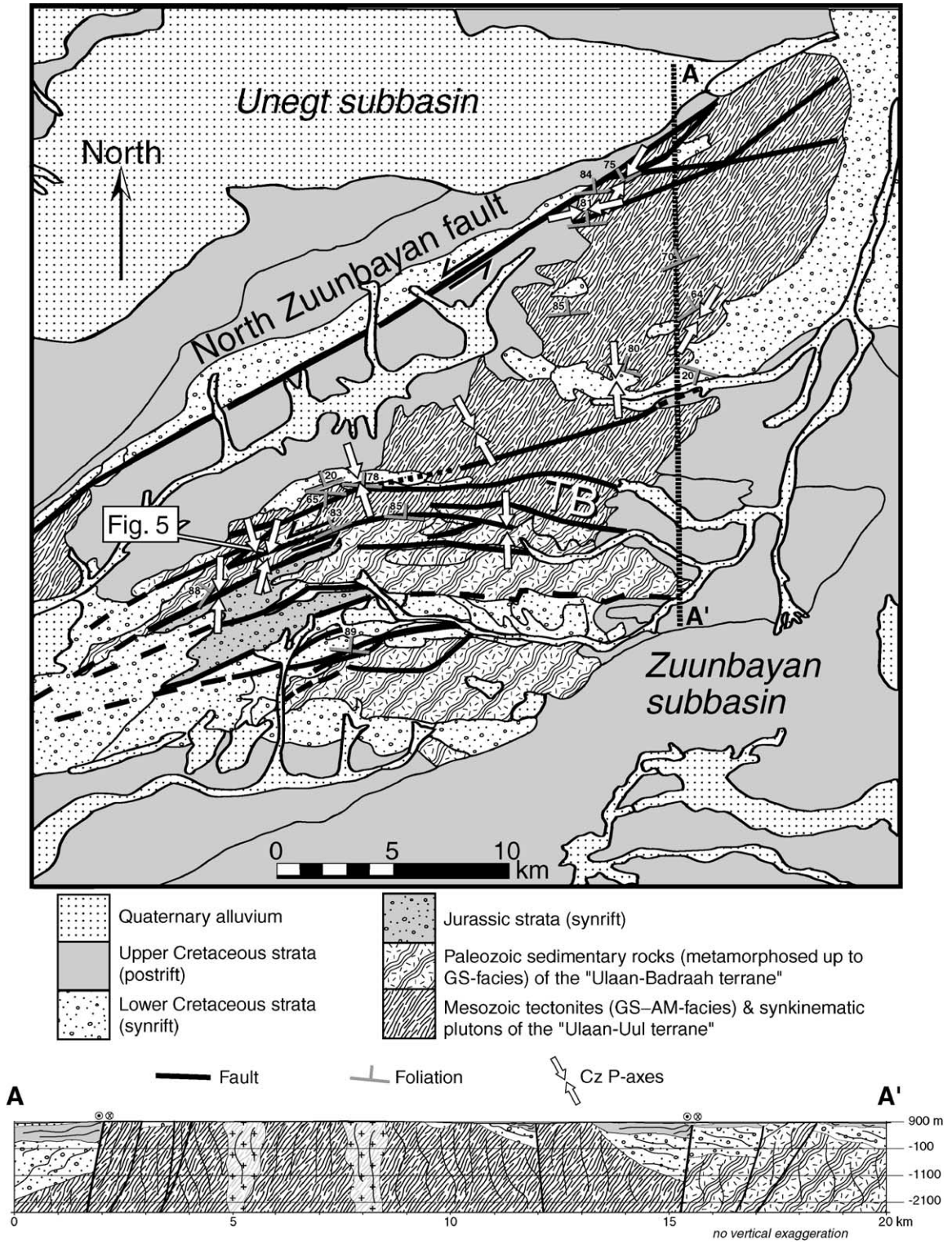

Fig. 3. Geologic map and schematic cross section of the Tavan Har field area. The map is simplified from Carson et al. [27] and from unpublished mapping by B. Bayanmonh. TB = inferred terrane boundary. Location of Fig. 5 photos is shown. Foliation symbol reflects strike and dip of bedding where shown in Mesozoic sedimentary units.

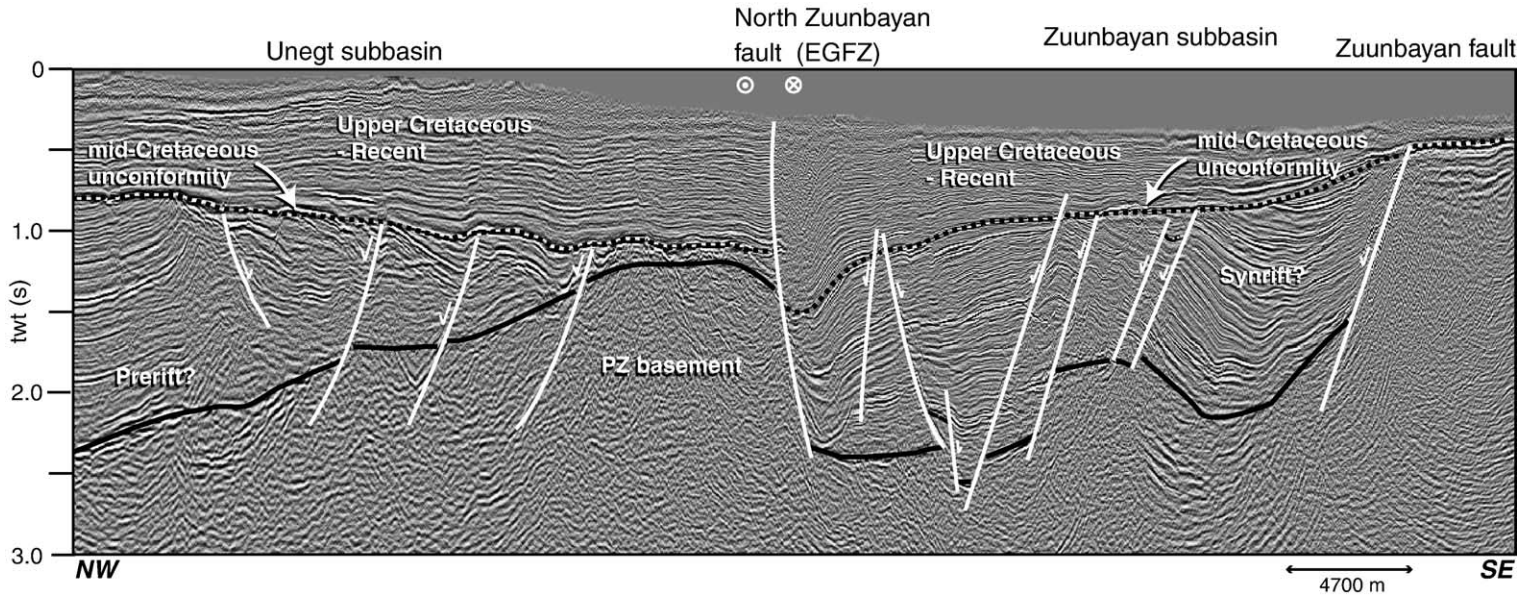

Fig. 4. Interpretation of a regional 2D seismic reflection profile across the Unegt and Zuunbayan subbasins modified after Johnson [5]. Vertical axis is in two-way travel time (s). Location of profile shown in Fig. 2. Note that the profile is across what appears to be a pull-apart basin in the left-lateral left-stepping fault system. This interpretation is consistent with the apparent normal sense offset seen across the North Zuunbayan fault in the profile.

phases, deformation was mainly concentrated along the EGFZ and the fault zone likely controlled regions of uplift and subsidence reflected in adjacent basin fill [5].

Paleozoic rocks of southern Mongolia record continental growth through accretion of volcanic arcs, associated marine basins, and, perhaps, fragments of continental crust [13,14]. These constituents accreted by the Late Permian during closure of a remnant ocean basin along the northern margin of the North China block [1,12]. Paleozoic rocks of southeastern Mongolia are particularly important in the context of this study because they comprise the basement upon which subsequent Mesozoic–Cenozoic deformation is superposed. In several places, faults of the EGFZ are mapped as a Paleozoic arc or terrane boundary (e.g., Fig. 4), mainly because of differences in metamorphic grade across the fault zone, but lack supporting age data. This may in fact represent a fundamental crustal boundary inherited from the Paleozoic, but alternatively could reflect juxtaposition via strike-slip faulting.

Metamorphic tectonites within the EGFZ, traditionally mapped as Precambrian basement (Fig. 1b), comprise a suite of synkinematic intrusions, amphibolite-facies gneisses and greenschist-facies mylonites that define an Early Mesozoic sinistral shear zone [3,15]. The shear zone is dominated by steeply dipping NE-trending foliations and subhorizontal stretching lineations. At higher structural levels, variably metamorphosed Paleozoic sedimentary sequences are caught up in discrete zones of mylonitic deformation. We have documented the ductile shear zone at several localities over a distance of 250 km along strike within the EGFZ (southern Tsagan Subarga, Tavan Har, and Urgun; Fig. 1b). In addition to one $^{40}Ar/^{39}Ar$ weighted mean age of 209 ± 2 Ma on biotite from mylonite [3], regional overlap relations also suggest a Late Triassic to Late Jurassic age of movement on these and other northeast-trending faults within Mongolia [8]. High-angle fabrics associated with gneissic and mylonitic foliations were exploited by subsequent deformation events in the brittle–ductile and brittle regimes.

The shear zone was reactivated by rift-related faulting during Early Cretaceous NW–SE-extension that also resulted in core complex formation at near the southern limit of the EGFZ along the Chinese–Mongolia border [15,16] (locality OH, Fig. 1b). Seismic data and correlated outcrop mapping at Tavan Har (Figs. 3 and 4) indicate that this major basin-dividing fault zone was active during Jurassic–Cretaceous time, and that rift basin formation was followed by basin inversion at c. 100–95 Ma [5].

An Upper Cretaceous–Recent post-rift megasequence lies unconformably on inverted Upper Mesozoic rift sequences [4]. The distribution of Cenozoic strata in the southeast Gobi is uncertain. Compared to older versions of geologic maps for the region (e.g., [17]), more recent versions depict relatively large swaths of Paleogene sediments within the EGFZ [8] (Fig. 1b). Cenozoic volcanic rocks are documented to the northeast of the field area along the Chinese–Mongolian border (Fig. 1a). Satellite images and maps show that the Dariganga volcanic field is spatially correlated with a series of NE-striking faults but is not cut by them (e.g., [8]). To our knowledge, there is no documentation of the volcanic rocks having been deformed. The age of the Dariganga volcanic field is typically quoted as Neogene–Quaternary, with some sparse radiometric age data suggesting eruption ages between ca. 14 and 1.6 Ma and major eruptive activity younger than 5 Ma ([18] and references within).

2. Cenozoic deformation in southeastern Mongolia

2.1. Subsurface data

While regional maps traditionally show very little Cenozoic sedimentation in the East Gobi basin, seismic reflection data clearly indicate that the mid-Cretaceous unconformity surface itself is deformed, and overlying strata are folded along the North Zuunbayan fault in the Tavan Har region of the EGFZ (Fig. 4; [5]). As it is imaged in the subsurface, the EGFZ consists of near-vertical structures that juxtapose distinct seismic sequences and is characterized by sudden along-strike changes in both the amount and sense of apparent offset. Such features are common to the subsurface expression of strike-slip faults in other regions [19]. The subsurface data therefore reveal that faults within the EGFZ both offset and deform post-rift Upper Cretaceous strata, indicating some degree of post Late Cretaceous fault activity.

2.2. Structural methods

Field evidence for Cenozoic faulting was identified at Ulgay Khid, Tsagan Subarga, Tavan Har, and Urgun blocks (Fig. 2). We conducted geologic transects across the structural grain of the EGFZ and complementary studies of geologic maps, satellite images, and digital elevation data. Orientations of fault planes and striae were recorded, along with details regarding the fault surface, overprinting relationships, and the age and nature of the rock types faulted (e.g., Fig. 5a). Sense

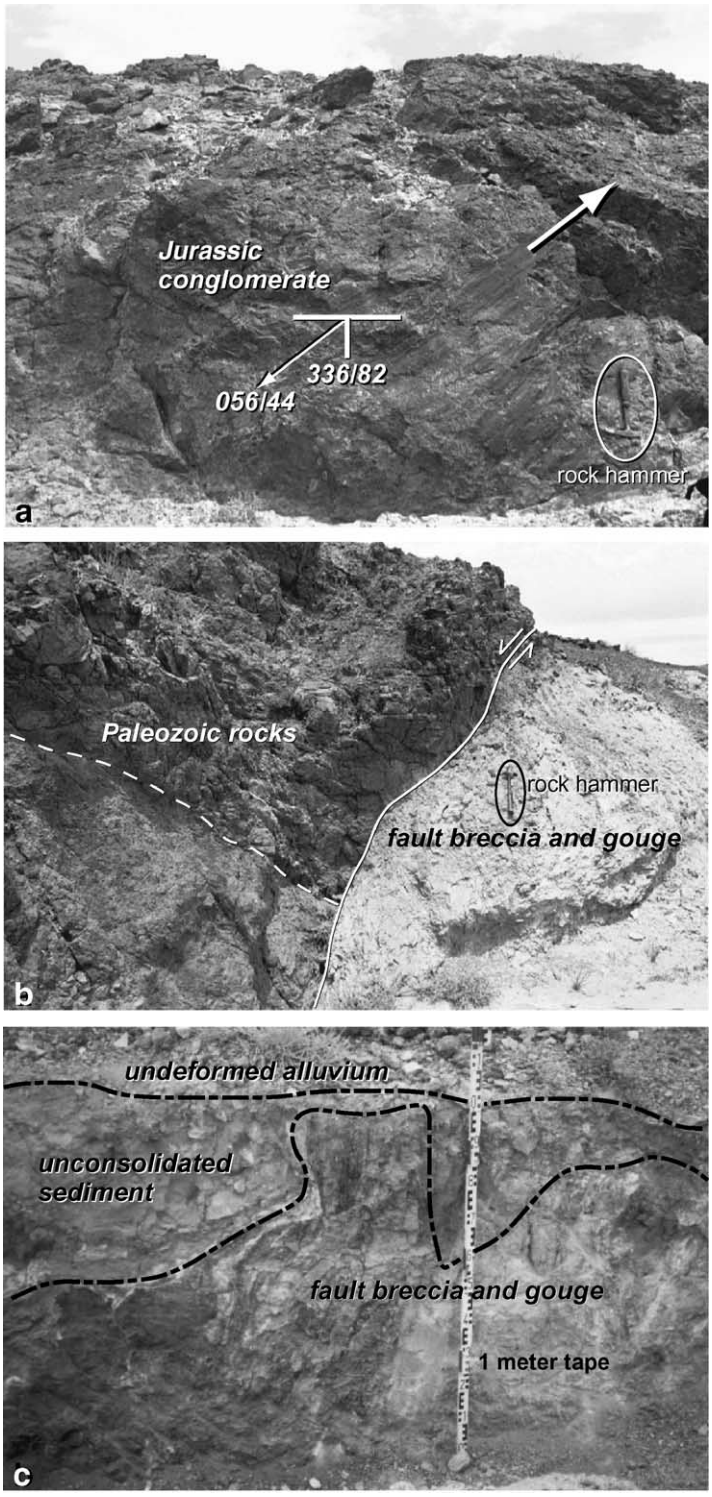

Fig. 5. Field photographs of Cenozoic faults at a Tavan Har locality. Location of photos is shown in Fig. 3. a) Footwall surface of a fault cutting a Jurassic conglomerate unit with slickensides. In the reference frame of the photograph, motion of the hanging wall was up and to the right (sinistral-oblique) as evidenced by steps on the fault plane. Symbol shows the measured dip direction and dip of the fault surface and the trend and plunge of the striae. Standard geologist's rock hammer is shown for scale. b) Sinistral fault cutting an older, highly oblique fault plane in Paleozoic rocks (dashed white line denotes trace of fault on outcrop). Standard geologist's rock hammer is shown for scale. c) Wall of a trench through one of the Cenozoic fault splays. Exposure demonstrates unconsolidated Cenozoic sediments involved in deformation and overlapped by undeformed alluvium.

of slip was deduced based on offset markers or features on the fault plane such as steps, Riedel shears, or fibers. Fault-slip data were weighted based on a confidence level regarding the sense of slip. Degrees of certainty (certain, probable, inferred, and unknown) are expressed by the style of arrowheads (filled, open, half, and headless, respectively) used in the stereonet plots (Fig. 2).

Because of multiple faulting episodes in the EGFZ, fault-slip data were evaluated in terms of the likelihood of representing "synrift", "inversion", or "Cenozoic" slip events and then pooled accordingly. These classifications were to some degree part of an iterative sorting process in which subsets of data were not allowed to violate relative age relationships observed in outcrop. In total, 260 fault-slip data were collected out of which 104 were ultimately classified as Cenozoic based on the fact that i) the faults either directly cut Upper Cretaceous or younger sedimentary rocks ($n=9$), or ii) were inferred to be kinematically related ($n=95$). We note that correlations took into account the association of calcite fibers on inferred Cenozoic fault planes and calcite filled fracture sets cutting Upper Cretaceous and younger sedimentary rocks, whereas Cretaceous faulting was more strongly associated with quartz and limonite coatings.

Computer programs from Sperner et al., [20] and Sperner and Ratschbacher [21] were utilized in the analysis of data subsets to calculate "stress axes" via the pressure–tension method (PBT; [22]) and "reduced stress tensors" via numerical dynamic analysis (NDA; [23]). The NDA program recognizes when glide sense of observed data is different from that calculated for the pooled data. Although faults with incompatible slip sense are retained in the stereonet plots, they were eliminated from NDA calculations. NDA calculates a fluctuation factor (F) which represents the average angle between orientations of the measured striae and the calculated shear stress. We refer the reader to Angelier [24] and Twiss and Unruh [25] for a discussion and critical evaluation of these techniques.

2.3. Surficial observations

Cenozoic faults control the present day topographic expression of basement blocks within the EGFZ. Map scale faults are dominated by northeast-trending, left-stepping, sinistral faults that exploit the previously existing structural grain of the EGFZ (Fig. 2). Direct field evidence for reactivation of pre-existing structural features included observation of multiple (incompatible) slip events on single fault planes, and sinistral slip associated with subhorizontal striae and calcite fibers on foliation planes of Mesozoic tectonites. Field data, regional maps, and digital elevation models suggest a higher prevalence of conjugate, NW-trending dextral strike-slip faults in the southwestern portion of the study area in the Ulgay Khid and Tsagan Subarga blocks (Fig. 2). The surface geology of these basement blocks is dominated by Paleozoic and Mesozoic sedimentary and volcanic rocks and, thus, represents higher structural levels than the Mesozoic tectonites of Tavan Har and Urgun. This observation is interpreted to reflect the likelihood that neo-formed Cenozoic faults were largely limited to regions lacking the strong NE-trending fabric related to the Mesozoic ductile shear zone.

Overall, results from inversion of Cenozoic fault-slip data sets for Ulgay Khid, Tsagan Subarga, Tavan Har, and Urgun blocks yielded results consistent with NNW–SSE horizontal shortening and ENE–WSW horizontal extension. Map projections of PBT P-axes for individual localities are plotted as arrows on Fig. 2. The NDA and PBT results for compiled data for each basement block are shown with faults on lower hemisphere equal area stereonets in Fig. 2 and results are tabulated in Table 1. The anisotropic nature of the geology upon which Cenozoic faulting was superposed violates primary assumptions required by stress inver-

Table 1
Results of fault-slip analyses for grouped data

Locality	NDA								Turner				
	σ_1	σ_2	σ_3	R	F	nev	n	θ	P	B	T	θ	n
UK	17010	06654	26734	0.33	17	4	36	30	16509	02778	26706	30	36
TS	34208	17282	07202	0.45	24	4	22	30	34200	07378	25312	30	22
TH	19006	33383	09904	0.47	21	13	39	30	18018	34571	08704	30	39
UR	36027	20162	09409	0.64	36	1	7	30	34410	21674	09309	30	7

See Methods section in text for full explanation.

Abbreviations and symbols not defined in text and used here include: UK = Ulgay Khid; TS = Tsagan Subarga; TH = Tavan Har; UR = Urgun; R = "stress ratio" = $(\sigma_2-\sigma_3)/(\sigma_1-\sigma_3)$; nev = number of data rejected by NDA; n = total number of data included in analyses; θ = internal angle of friction used in calculations.

sions and therefore the results for the Cenozoic fault-slip data sets are interpreted herein only in terms of kinematics rather than paleostress in its strict dynamic sense. There is reasonably good agreement, with a few obvious exceptions, regarding the orientation of the majority of PBT axes calculated for individual localities as well as those indicated by PBT and NDA calculations for the bulk Cenozoic data sets from each basement block. The calculated fluctuation factors (F) range from 17° to 36°, thereby implying heterogeneous data sets (homogeneous fault populations will tend to have an F value of $\leq 10°$; see Ratschbacher et al. [26] and references therein). This result is not entirely unexpected and may reflect local aberrations due to local fault interactions as well as the preferential reactivation of pre-existing structures. These data should not be over-interpreted, but the consistency of results suggests that they are meaningful with respect to the Cenozoic kinematics of the fault zone.

Regional maps of Tavan Har divide the block into two different basement types; the juxtaposition has been interpreted as a Paleozoic terrane boundary ([27]; Fig. 4). Rocks of the northern half of Tavan Har comprise mylonite, schist, gneiss, and synkinematic intrusives. Though mapped as part of the Proterozoic 'Ulaan-Uul' terrane [27], these rocks are in fact metamorphic tectonites of the Late Triassic sinistral shear zone. The southern half of Tavan Har has been mapped as the 'Hovsgol-Ulaanbadrah' terrane and includes greenschist-grade Paleozoic sedimentary rocks and intrusive complexes. These rocks also record evidence of Late Triassic sinistral shear just south of the mapped terrane boundary [15]. Field mapping reveals that the inferred terrane boundary is in fact one of two major brittle sinistral strike-slip faults that define the EGFZ at Tavan Har. The North Zuunbayan fault was identified in the subsurface by Johnson [5] and defines the northern topographic limit of the Tavan Har block. The southern 'terrane boundary' fault zone consists of subparallel fault strands continuous for more than 13 km (mapped length) that splay to the east. Fault gouge, breccia, and slivers of Paleozoic basement rocks are associated with fault strands that define a zone 10s to 100s of meters wide. The fault zone itself does not have a clear surface expression (i.e., modern fault scarp) except that resulting from erosion (e.g., Fig. 5b).

Trenching along the southern fault strand revealed clay and powder-sized fault gouge and breccia, in multiple zones 1–10 m wide. These zones have variable color (pink, gray, white, black), and common white calcite veins. Most significantly, trenches reveal faults with gouge that cross-cut and deform unconsolidated sediment (Fig. 5c), which includes poorly sorted calcareous sand and gravel. An undisturbed layer of unconsolidated sediment overlaps both the gouge and deformed sediment zones. This undeformed layer forms the modern pavement surface of rock-varnished gravel–cobble alluvium common to the area.

Lithologies within the unconsolidated alluvium have not yet yielded radiometric or spore/pollen dates. However, Upper and Lower Cretaceous strata are widespread and well-studied in the region and, by comparison, bear little resemblance to the units found in the trenches. Upper Mesozoic strata in the region are generally well-cemented and lithified due to burial of up to 1–2 km, and include lacustrine shale and carbonate, abundant volcanics, and alluvial–fluvial lithofacies assemblages [4,28]. Alluvium found in the fault zone lacks the distinctive red color of Upper Cretaceous strata in much of the southeastern Mongolia, which also tend to be better lithified than what is seen in the fault zone. The unconsolidated sediment found within the breccia and gouge zones therefore postdates the Upper Cretaceous post-rift sequence, and is most likely Cenozoic in age.

3. Discussion

Outcrop and subsurface data support a Cenozoic phase of deformation in the EGFZ involving strike-slip faulting. One previous study [9] cites post-Cretaceous dextral motion on northeast-trending faults in the area. That interpretation, however, appears to be based on limited, medium to low confidence data. Alternatively, those observations may reflect a more recent and limited phase of faulting (see discussion to follow). Our fault-slip data from several basement block localities within the EGFZ indicate, rather, that regional Cenozoic faulting was dominated by sinistral strike-slip faulting on northeast-trending structures. Conjugate dextral faults appear to play only a minor role, possibly due to the inherited NE-trending structural grain of the EGFZ.

The fault-slip inversions yielded P-axes at higher angles to the mapped faults than typically expected for strike-slip fault systems. It is important to emphasize that these faults did not form in response to an imposed Cenozoic stress field but, rather, are reactivated structures. While we do not interpret the inversion data presented here to represent principal stress directions, it is probably a fair assumption that if the calculated shortening and extension axes for each of the

grouped sets of fault-slip data and the majority of individual localities are subhorizontal (Fig. 2), then σ_1 and σ_3 were likely subhorizontal as well. Thus, the possibility exists that blocks within the EGFZ may have experienced vertical axis rotations. With progressive faulting, "*P*-axes" (as recorded by the fault-slip data) may have rotated counterclockwise to a higher-angle orientation to the regional faults. Many of the fault-slip data, however, do show a dip-slip component and are consistent with an element of transpression (Figs. 2 and 5a) and so σ_1 may also have been highly oblique to the pre-existing structural trends within the EGFZ.

3.1. Comparison with neotectonic framework

The apparent NNW-shortening and ENE-extension directions implied by Cenozoic fault-slip data in the study area are incompatible with most studies regarding neotectonics of Asia (e.g., [29–31]). Inversions of Cenozoic fault-slip data from the EGFZ yield axes nearly orthogonal to those calculated by these studies. However, there is not complete agreement with respect to the implications of geodetic data available for this region. Calais and Amarjargal [32] and Calais et al. [33] record the relative eastward motion of the Amurian/North China block relative to stable Eurasia. These data require the presence of left-lateral faulting to the north of the study area, and this motion is likely taken up by extension at Lake Baikal and the left-lateral Stanovoy fault system that extends from its northern end toward the Sea of Okhotsk [29,34,35]. Conversely, Shen et al. [36] infer the presence of left-lateral faulting along the northern rim of China based on GPS data that show China to be moving eastward relative to "stable" Mongolia. Although there are apparently conflicting views as to whether the EGFZ should be included as part of stable Eurasia or not, the data from Mongolia seem to weigh more heavily in favor of its motion relative to Eurasia [32,33].

Compiled twentieth century seismicity data for Mongolia [37] reveal that the EGFZ is located in one of the least seismically active areas of Mongolia. The EGFZ region experienced several earthquakes of magnitude 6.5 or below between 1900 and 2000, but earthquakes were sporadic and the region stands in stark contrast to the western portion of the country where the active faults are clearly defined by continuous clustering of earthquake epicenters. These data in conjunction with our observations above lead us to propose a Tertiary age for regional Cenozoic faulting in southeastern Mongolia.

3.2. Tectonic implications

The recognition of Tertiary faulting along the EGFZ has broad implications that extend well beyond the regional geology. These results are relevant to models regarding continental deformation associated with the Indo-Asia collision as to whether convergence has been accommodated by plane strain, plate-like deformation resulting in extrusion of coherent lithospheric blocks (e.g. [11]) versus continuum crustal thickening (e.g., [10]), or some combination of the two in which the former transitions to the latter [38].

The Altyn Tagh fault (ATF; Fig. 1) is a topic of ongoing debate. Some studies of offset of pre-Tertiary geologic features have indicated a total displacement of approximately 375 km on the ATF, largely in Oligocene–Miocene time [39,40]. Yin et al. [41], however, suggest 470 km of Cenozoic offset with strike-slip faulting initiating at c. 49 Ma. Several authors have proposed the extension of the ATF northeastward through the EGFZ and beyond to the Sea of Okhotsk (e.g., [35,38,42]). Others consider the fault to terminate by linking with thrust faults in the region of the Qilian Shan at the northern edge of the Tibetan Plateau (e.g., [41,43,44]). At the heart of this debate, in our opinion, is not whether slip on the ATF is transferred to these thrusts faults today, but the feasibility of the ATF having once transferred left-lateral slip to faults north of the Qilian Shan (i.e. having been kinematically linked with the EGFZ). The possibility of the latter requires first that the presence of a linking system of faults between the present day northern termination of the ATF and the EGFZ be identified. Secondly, it requires that these faults have compatible history prior to the onset of thrusting in the Qilian Shan, for which estimates range from 20–10 Ma [45] to after 6–5 Ma [46].

New observations from the Alxa fault zone area document the presence of Cenozoic sinistral strike-slip activity on roughly E–W trending faults, bridging the gap between the ATF and the Mongolian border (Fig. 1; [47]). These workers estimate post-Cretaceous offsets in the range of tens of kilometers to greater than 150 km, noting limited Neogene displacement. Various piercing points have been proposed for the Alxa–EGFZ near the Mongolia–China border but as of yet have not been rigorously tested. For example, Yue and Liou [38] proposed some 400 km of left-lateral offset beginning in the Late Oligocene (c.f. Yue et al. [48]). In contrast, Lamb et al. [3] proposed 185–235 km of offset in southeast Mongolia associated with Late Triassic sinistral shear (e.g. A–A′ and B–B″, Fig. 1b). In both cases,

these studies relied heavily on interpretations of regional maps but lacked complementary field campaigns. Given the evidence for left-lateral offset in both the Mesozoic and Cenozoic and the fact that offset was based on displaced Paleozoic rocks, the proposed piercing points in both cases can only represent total offset.

Remote sensing data indicate that multiple fault strands exist northeast of the Qilian Shan, suggesting that Cenozoic slip may have been distributed over several faults (Fig. 1b). We hypothesize that maximum slip magnitude along the EGFZ in the Cenozoic may have been as much as 150 km, similar to estimates for the Alxa region by Darby et al. [47]. In both regions, this magnitude is based on offset Early Cretaceous sedimentary basins. Comparative field studies of synrift strata at Tavan Har and Har Hotol support the inference from seismic data (Fig. 4) that very different sequences of Cretaceous and younger strata are juxtaposed by some amount of movement postdating their deposition. These observations include distinct sediment sources and overall stratigraphic architecture for Lower Cretaceous strata [4], which at Har Hotol (Fig. 1b) include distinctive red bed alluvial and fluvial units, basalt flows and reworked ash deposits, and freshwater lacustrine units. In contrast, synrift strata at Tavan Har include extensive and lithologically distinctive, organic-rich laminated mudstones locally termed 'paper shales.' While facies transitions are common over relatively short distances in nonmarine basins, our studies indicate that some of these lake systems were long-lived, widespread (e.g., >50 km) and stratified, and are actually truncated by the EGFZ [49]. North of the fault zone, the most likely lithologic match with paper shale units from Tavan Har occurs near Ulgay Khid (Fig. 1b, C–C′). Molecular organic geochemical studies also indicate similarities between distinctive lacustrine units at these localities [50]. Thus the sedimentary data would suggest that ~100–150 km of slip can be attributed to the Cenozoic deformation phase, pending further comparison of those units.

Field-based observations have thus been made toward satisfying the minimal requirements to support a Tertiary kinematic linkage between the ATF and EGFZ noted above (this work and Darby et al. [47]). These data potentially lend credence to the model of Yue and Liou [38] proposing a two-stage history in which sinistral faulting is transferred from the ATF to the EGFZ and associated faults beginning in Late Oligocene and transitions to thrusting in the Qilian Shan between 16 and 13 Ma. The proposed switch from transferred sinistral faulting (extrusion) to termination into thrust faults in the Qilian Shan (crustal thickening) roughly coincides with the transition along the northeastern Pacific margin from transtensional to transpressional tectonics believed to have occurred in the Late Miocene [35,42]. This fundamental switch in the boundary conditions related to the Pacific margin may explain why the EGFZ appears to have become relatively inactive compared to the Gobi Altai where faulting actively continues today.

4. Conclusions

New field observations from southeastern Mongolia testify to regional Cenozoic sinistral faulting on the NE-trending EGFZ. This deformation was associated with roughly NNW-shortening and ENE-extension. Lines of evidence that lead to a conservative estimate of a Tertiary age of faulting include interpreted seismic reflection data that reveal that the mid-Cretaceous unconformity is deformed by strike-slip faults [5] and field observations of strike-slip faults and fracture sets that cut Upper Cretaceous and Cenozoic strata but are overlapped by alluvial sediments that form the desert pavement. Additionally, seismicity maps argue against the presence of significant Quaternary faulting within the EGFZ. Cenozoic sinistral faulting along NE-trending structures in southeastern Mongolia was likely driven by the Indo-Asian collision and facilitated by Pacific margin transtension. A Middle Miocene or older linkage between the ATF and EGFZ appears increasingly feasible as more data become available. However, a rigorous campaign to constrain the timing and displacement associated with the Cenozoic EGFZ and related Asian faults is required to further evaluate such models. Nonetheless, the reactivation history of the EGFZ strongly supports the notion that inherited lithospheric structures are important in controlling the location and, thus, modes of intracontinental deformation.

Acknowledgements

This research was supported by the American Chemical Society, Petroleum Research Fund (grant 40193-G8 to C.L. Johnson) and benefited from National Science Foundation funding (grants EAR 9614555 and EAR-IF 0130833). Initial discovery and trenching of Cenozoic faults at Tavan Har took place during a field study supported in part by the Keck Consortium in July, 2003. A. Bayasgalan, B. Bayanmonh, R.J. Carson, P. Kast, N. Manchuk, K. Pogue, and other members of that field party contributed significantly to the initial studies of these structures in outcrop. M. Affolter con-

tributed to field studies in 2004. C. Minjin, N. Manchuk, and G. Sersmaa provided logistical support during 2004, as well as invaluable scientific guidance regarding Paleozoic stratigraphy and regional geology. We thank B. Darby, D. Cunningham, and an anonymous reviewer for comments that helped to improve the manuscript.

References

[1] J. Amory, Permian Sedimentation and Tectonics of Southern Mongolia, Stanford University, 1996.
[2] G. Badarch, W.D. Cunningham, B.F. Windley, A new terrane subdivision for Mongolia; implications for the Phanerozoic crustal growth of Central Asia, J. Asian Earth Sci. 21 (2002) 87–110.
[3] M.A. Lamb, A.D. Hanson, S.A. Graham, G. Badarch, L.E. Webb, Left-lateral sense offset of upper Proterozoic to Paleozoic features across the Gobi Onon, Tost, and Zuunbayan faults in southern Mongolia and implications for other Central Asian faults, Earth Planet. Sci. Lett. 173 (1999) 183–194.
[4] S.A. Graham, M.S. Hendrix, C.L. Johnson, D. Badamgarav, G. Badarch, J. Amory, M. Porter, R. Barsbold, L.E. Webb, B.R. Hacker, Sedimentary record and tectonic implications of late Mesozoic rifting, southeast Mongolia, Geol. Soc. Amer. Bull. 113 (2001) 1560–1579.
[5] C.L. Johnson, Polyphase evolution of the East Gobi basin: sedimentary and structural records of Mesozoic–Cenozoic intraplate deformation in Mongolia, Basin Res. 16 (2004) 79–99.
[6] A. Bayasgalan, J. Jackson, J.-F. Ritz, S. Carretier, Field examples of strike-slip fault terminations in Mongolia, and their tectonic significance, Tectonics 18 (1999) 394–411.
[7] D. Cunningham, A.H. Dijkstra, J. Howard, A. Quarles, G. Badarch, Active intraplate strike-slip faulting and transpression uplift in the Mongolian Altai, Geol. Soc. Spec. Pub. 210 (2003) 65–87.
[8] O. Tomurtogoo, Geological Map of Mongolia, Map Scale 1:1,000,000, General Directorate of Mineral Research and Exploration, Ankara, Turkey, 1999.
[9] G. Prost, Tectonics and hydrocarbon systems of the East Gobi basin, Mongolia, Am. Assoc. Pet. Geol. Bull. 88 (2004) 485–513.
[10] G. Houseman, P. England, A lithospheric-thickening model for the Indo-Asian collision, in: A. Yin, M. Harrison (Eds.), The Tectonic Evolution of Asia, Cambridge University Press, Cambridge, 1993, pp. 3–17.
[11] P. Tapponnier, G. Peltzer, A.Y. Le Dain, R. Armijo, P. Cobbold, Propagating extrusion tectonics in Asia; new insights from simple experiments with Plasticine, Geology 10 (1982) 611–616.
[12] J.J. Traynor, C. Sladen, Tectonic and stratigraphic evolution of the Mongolian People's Republic and its influence on hydrocarbon geology and potential, Mar. Pet. Geol. 12 (1995) 35–52.
[13] A.M.C. Sengor, B.A. Natal'in, V.S. Burtman, Evolution of the Altaid tectonic collage and Palaeozoic crustal growth in Eurasia, Nature 364 (1993) 299–307.
[14] M.A. Lamb, G. Badarch, Paleozoic sedimentary basins and volcanic-arc systems of southern Mongolia; new stratigraphic and sedimentologic constraints, Int. Geol. Rev. 39 (1997) 542–576.
[15] L.E. Webb, C.L. Johnson, C. Minjin, G. Sersmaa, M. Affolter, N. Manchuk, Mesozoic and Cenozoic intracontinental deformation in southeastern Mongolia, in: Eos Transactions, AGU, 2004 Fall Meeting Supplemental Abstracts, vol. 85 (47), 2004, p. F1698.
[16] L.E. Webb, S.A. Graham, C.L. Johnson, G. Badarch, M.S. Hendrix, Occurrence, age, and implications of the Yagan-Onch Hayrhan metamorphic core complex, southern Mongolia, Geology 27 (1999) 143–146.
[17] A.L. Yanshin, Geologic Map of the Mongolian People's Republic, Map Scale 1:1,500,000, Akad, Nauk USSR, Moscow, 1989.
[18] V.A. Kononova, G. Kurat, A. Embey-Isztin, V.A. Pervov, C. Koeberl, F. Brandstaetter, Geochemistry of metasomatised spinel peridotite xenoliths from the Dariganga Plateau, south-eastern Mongolia, Min. Pet. 7 (2002) 1–21.
[19] G. Zolnai, Continental wrench-tectonics and hydrocarbon habitat [revised], in: Amer. Assoc. of Petrol. Geol. Continuing Ed. Course Note Ser., vol. 30, 1991, pp. 1–304.
[20] B. Sperner, L. Ratschbacher, R. Ott, Fault-striae analysis: a Turbo Pascal program package for graphical representation and reduced stress-tensor calculation, Comput. Geosci. 19 (1993) 1361–1388.
[21] B.R. Sperner, L. Ratschbacker, A Turbo Pascal program package for graphical representation and stress analysis of calcite deformation, Z. Dtsch. Geol. Gesell. 145 (1994) 414–423.
[22] F.J. Turner, Nature and dynamic interpretation of deformation lamellae in calcite of three marbles, Am. J. Sci. 251 (1953) 276–298.
[23] J.H. Spang, Numerical method for dynamic analysis of calcite twin lamellae, Geol. Soc. Amer. Bull. 83 (1972) 467–472.
[24] J. Angelier, Fault-slip analysis and paleostress reconstruction, in: P.L. Hancock (Ed.), Continental Deformation, Pergamon, Tarrytown, NY, 1994, pp. 53–100.
[25] R.J. Twiss, J.R. Unruh, Analysis of fault slip inversions: do they constrain stress or strain rate?, J. Geophys. Res. 103 (1998) 12,205–212,222.
[26] L. Ratschbacher, W. Frisch, H.-G. Linzer, B. Sperner, M. Meschede, K. Decker, J. Nemčok, R. Grygar, The Pieniny Klippen Belt in the western Carpathians of northeastern Slovakia: structural evidence for transpression, Tectonophysics 226 (1993) 471–483.
[27] R.J. Carson, B. Bayanmonh, A. Bayasgalan, C.L. Johnson, K.R. Pogue, K.W. Wegmann, Geology of the Tavan Har area, Gobi, Mongolia, in: A. Ewing (Ed.), Seventeenth Annual Keck Research Symposium in Geology, Keck Geology Consortium, Northfield (MN), 2004, pp. 170–175.
[28] C.L. Johnson, S.A. Graham, Sedimentology and reservoir architecture of a synrift lacustrine delta, southeastern Mongolia, J. Sediment. Res. 74 (2004) 770–785.
[29] G. Peltzer, F. Saucier, Present-day kinematics of Geological Society of America Asia derived from geologic fault rates, J. Geophys. Res. 101 (1996) 27,943–927,956.
[30] E. Calais, O. Lesne, J. Deverchère, V. Sankov, A. Lukhnev, A. Miroshnitchenko, V. Buddo, K. Levi, V. Zalutzky, Y. Bashkuev, GPS measurements of crustal deformation in the Baikal rift zone, Siberia, Geophys. Res. Lett. 25 (1998) 4003–4006.
[31] L.M. Flesch, A.J. Haines, W.E. Holt, Dynamics of the India–Eurasia collision zone, J. Geophys. Res. 105 (2001) 16,435–416,460.
[32] E. Calais, S. Amarjargal, New constraints on current deformation in Asia from continuous GPS measurements at Ulan Bataar, Mongolia, Geophys. Res. Lett. 27 (2000) 1527–1531.

[33] E. Calais, M. Vergnolle, V. Sankov, A. Lukhnev, A. Miroshnitchenko, S. Amarjargal, J. Deverchère, GPS measurements of crustal deformation in the Baikal–Mongolia area (1994–2002): implications for current kinematics of Asia, J. Geophys. Res. 108 (2003) B10, 2501, doi:10.1029/2002JB002373.

[34] K. Fujita, F.W. Cambray, K.G. Mackey, B.M. Kozmin, V.S. Imaev, B.P. Vazhenin, V.N. Kovalev, W.Y. Chung, H. Gao, Seismotectonics of eastern Russia: from Baikal to Chukotka, Abstr. Programs - Geol. Soc. Am. 27 (5) (1995) 19.

[35] D.M. Worrall, V. Kruglyak, F. Kunst, V. Kuznetsov, Tertiary tectonics of the Sea of Okhotsk, Russia: far-field effects of the India–Eurasia collision, Tectonics 15 (1996) 813–826.

[36] Z.-K. Shen, C. Zhao, A. Yin, Y. Li, D. Jackson, P. Fang, D. Dong, Contemporary crustal deformation in east Asia constrained by global positioning system measurements, J. Geophys. Res. 105 (2000) 5721–5734.

[37] A.M. Ankhtsetseg, Ts. Baasanbat, G. Bayar, Ch. Bayarsaikhan, D. Erdenezul, D. Mungunsuren, A. Munkhsaikhan, D. Munkhuu, R. Narantsetseg, Ch. Odonbaatar, L. Selenge, B. Tsembei, M. Ulzübat, Kh. Urtnasan, One century of seismicity in Mongolia (1900–2000), Res. Cent. Astron. and Geophys., Mongolian Acad. Sci., Ulaan Bataar, Mongolia, 2003.

[38] Y. Yue, J.G. Liou, Two-stage evolution model for the Altyn Tagh fault, China, Geology 27 (1999) 227–230.

[39] B.D. Ritts, U. Biffi, Magnitude of post-Middle Jurassic (Bajocian) displacement on the Altyn Tagh fault, NW China, Geol. Soc. Amer. Bull. 112 (2000) 61–74.

[40] Y. Yue, B.D. Ritts, S.A. Graham, Initiation and long-term slip history of the Altyn Tagh fault, Int. Geol. Rev. 43 (2001) 1087–1093.

[41] A. Yin, P.E. Rumelhart, R. Butler, E. Cowgill, T.M. Harrison, D.A. Foster, R.V. Ingersoll, Q. Zhang, X.-F. Wang, A. Hanson, A. Raza, Tectonic history of the Altyn Tagh fault system in northern Tibet inferred from Cenozoic sedimentation, Geol. Soc. Amer. Bull. 114 (2002) 1257–1295.

[42] L. Jolivet, K. Tamaki, M. Fournier, Japan Sea, opening history and mechanism—A synthesis, J. Geophys. Res. 99 (1994) 22,237–222,259.

[43] A. Yin, S. Nie, A Phanerozoic palinspastic reconstruction of China and its neighboring regions, in: A. Yin, M. Harrison (Eds.), The Tectonic Evolution of Asia, Cambridge University Press, Cambridge, 1996, pp. 442–485.

[44] A. Yin, T.M. Harrison, Geologic evolution of the Himalayan–Tibetan orogen, Annu. Rev. Earth Planet. Sci. 28 (2000) 211–280.

[45] A. George, S.J. Marshallsea, K.-H. Wyrwoll, J. Chen, Y. Lu, Miocene cooling in the northern Qilian Shan, northeastern margin of the Tibetan plateau, revealed by apatite fission-track and vitrinite reflectance analysis, Geology 29 (2001) 939–942.

[46] B.C. Burchfiel, D. Quidong, P. Molnar, L. Royden, W. Yipeng, Z. Peizhen, Z. Weiqi, Intracrustal detachment zones of continental deformation, Geology 17 (1989) 448–452.

[47] B.J. Darby, Ritts, B.D., Yue, Y., and Meng, Q., Did the Altyn Tagh fault extend beyond the Tibetan Plateau? Earth and Plan. Sci. Lett. (in press).

[48] Y. Yue, J.G. Liou, S.A. Graham, Tectonic correlation of Beishan and Inner Mongolia orogens and its implications for the palinspastic reconstruction of North China, Mem.—Geol. Soc. Amer. 194 (2001) 101–116.

[49] C.L. Johnson, S.A. Graham, Sedimentology and reservoir architecture of a synrift lacustrine delta, southeastern Mongolia, J. Sediment. Res. 74 (2004) 770–785.

[50] C.L. Johnson, T.J. Greene, D.A. Zinniker, J.M. Moldowan, M.S. Hendrix, A.R. Carroll, Geochemical characteristics and correlation of oil and nonmarine source rocks from Mongolia, AAPG Bull. 87 (2003) 817–846.